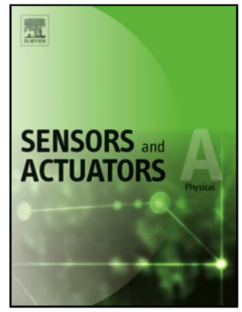

Title: Metglas thin film based magnetostrictive transducers for use in long period fibre grating sensors

Authors: Senoy Thomas, Jinesh Mathew, P. Radhakrishnan, V.P.N. Nampoori, A.K. George, S.H. Al-Harthi, R.V. Ramanujan, M.R. Anantharaman

PII:	S0924-4247(10)00219-0
DOI:	doi:10.1016/j.sna.2010.05.006
Reference:	SNA 6979

To appear in: *Sensors and Actuators A*

Received date:	16-12-2009
Revised date:	10-3-2010
Accepted date:	11-5-2010

Please cite this article as: S. Thomas, J. Mathew, P. Radhakrishnan, V.P.N. Nampoori, A.K. George, S.H. Al-Harthi, R.V. Ramanujan, M.R. Anantharaman, Metglas thin film based magnetostrictive transducers for use in long period fibre grating sensors, *Sensors and Actuators: A Physical* (2008), doi:10.1016/j.sna.2010.05.006

Metglas thin film based magnetostrictive transducers for use in long period fibre grating sensors

Senoy Thomas[1,$], Jinesh Mathew [2, #], P. Radhakrishnan[2], V. P. N. Nampoori[2], A. K. George[3], S.H. Al-Harthi[3], R. V. Ramanujan[4] and M. R. Anantharaman[1,*]

[1]Department of Physics, Cochin University of Science and Technology, Cochin-682022, India

[2]International School of Photonics, Cochin University of Science and Technology, Cochin-682022, India

[3]Department of Physics, Sultan Qaboos University, Muscat, Sultanate of Oman

[4]School of Materials Science and Engineering, Nanyang Avenue, Nanyang Technological University, Singapore 639798, Singapore

[$]Presently at Institute for Physics, Technical University of Chemnitz, D-09107 Chemnitz, Germany

[#]Presently at Photonics Research Centre, School of Electronic and Communications Engg., Dublin Institute of Technology, Ireland

* Author to whom correspondence should be addressed, E-mail: mraiyer@gmail.com

Abstract

Metallic glass alloy Metglas 2826 MB based amorphous magnetic thin films were fabricated by the thermal evaporation technique. Transmission electron micrographs and electron diffraction pattern showed the amorphous nature of the films. Composition of the films was analyzed employing x-ray photoelectron spectroscopy and energy dispersive x-ray spectroscopy techniques. The film was integrated to a long period fibre grating. It was observed that the resonance wavelength of the fibre grating decreased with an increase in the magnetic field. Change in the resonance wavelength was minimal at higher magnetic fields. Field dependent magnetostriction values revealed the potential application of these films in magnetostrictive sensor devices.

Keywords: Metglas thin films, Long period fibre grating, magnetostrictive sensors, thermal evaporation, x-ray photoelectron spectroscopy, amorphous magnetic materials

I. Introduction

Magnetostrictive materials are currently of great interest due to their application potential in sensors and actuators [1-3]. Highly magnetostrictive materials are useful for ultrasound generators, magnetostrictive optical wavelength tuners and magnetostrictive delay lines [4]. Some of the requirements for practical applications of magnetostrictive materials include the capability to provide high saturation magnetostriction at low applied fields, ease of fabrication in a desired shape and low cost.

Metallic glass alloy Metglas 2826 MB based amorphous alloys are the best known candidates for magnetostrictive sensors because these amorphous alloys exhibit large saturation magnetostriction, high saturation magnetization, low anisotropy energies and low coercivity [5-7]. At present these alloys are available only in the form of ribbons of thickness ranging from 10 to 50 microns. A series of post treatment process such as high temperature annealing and epoxy treatment are further required for amorphous alloy ribbons to be used as sensors. Therefore there are many difficulties in fabricating systems based on amorphous ribbons for micro sensor applications. Magneto elastic materials in the form of thin films are an alternative to ribbons and they can be integrated easily in Micro Electro Mechanical Systems (MEMS) and Nano Electro Mechanical Systems (NEMS) [8]. This not only allows the miniaturization of sensor elements, but also enables the same micro-fabrication technologies to be used in the production of both electronic and magnetic devices. The integration of magnetic components into MEMS (MagMEMS) offers the advantages of implementing wireless technology [9]. In comparison with other MEMS technologies, for example those incorporating piezoelectric materials, MagMEMS offer a high power density, low performance degradation, fast response times and ease of fabrication.

Thin films based on metallic glasses can be prepared by techniques such as thermal evaporation, electrodeposition, molecular beam epitaxy, pulsed laser deposition and sputtering. Vapour deposition offers a simple alternative to sputter deposition in obtaining thin films of supersaturated solid solutions and other metastable states. Some attempts to prepare Metglas 2826 MB thin films by thermal evaporation have been reported in the literature [10-15]. Thin films of $Fe_{40}Ni_{38}Mo_4B_{18}$ were prepared by the flash evaporation technique [10]. Electron microscopy and diffraction investigations on these films showed that the films decompose in an eutectic fashion with thermal annealing. Magnetic studies were not carried out on these samples and the main focus of the paper was on the structural evolution of these films with thermal annealing. An alloy film deposited from a target of composition $Fe_{40}Ni_{38}Mo_4B_{18}$ was studied previously by our group [11-15]. When metglas thin films are grown it is necessary that their composition is determined as accurately as possible and technique like XPS is very useful in such studies. Moreover, the as prepared amorphous magnetic thin films usually present high coercivity due to stresses in the films. The magnetic property of such films strongly depends on the magnitude of magnetoelastic anisotropies. So the measurement of magnetostriction is also important in the study of the amorphous ferromagnetic thin films.

Optical fibre long period grating (LPG) can be utilized to quantify the magnetostriction in thin films. It is a non destructive technique. Optical fibre long period grating based sensing methods offer other advantages of electromagnetic interference immunity, compactness, ease of fabrication and multiplexing [16].

LPG's are usually fabricated by exposing the core of a photosensitive optical fibre to a spatially varying ultra-violet beam [17]. Typically, the impinging UV beam is periodic in space and results in a regular pattern of refractive index modulation in the fibre core. For these gratings the energy typically couples from the fundamental guided mode to discrete, forward propagating cladding mode. Each LPG with a given periodicity Λ selectively filters light in a narrow band width centered on the peak wavelength of coupling λ_i [18]

$$\lambda_i = \left[n_{eff}(\lambda_i) - n^i_{cladd}(\lambda_i)\right]\Lambda \qquad (1)$$

Where n_{eff} is the effective index of refraction of the propagating core mode, n^i_{cladd} is the index of refraction of the ith cladding mode, Λ is the period of grating and λ_i is the coupling wavelength. The value of n_{eff} depends on the core and cladding refractive index while the value of n^i_{cladd} depends on the core, cladding and air indices. When a tensile stress is applied to the optical fibre long period grating, the periodic spacing changes and thereby causes the coupling wavelength to shift. This provides a sensitive mechanism to measure the stress/strain and also the magnetostriction of a material attached to the fibre grating.

Few reports exist there in the literature describing the possible use of magnetostrictive transducers in fibre optic based sensors [19-21]. Miroslav Sedlar *et al.* [19] reported the magnetic field sensing properties of ferrite coated single mode optical fibers. Rengarajan and Walser [20] reported the fabrication of a high speed fibre optic sensor for magnetic field mapping. Their magnetostrictive transducer consisted of a multilayer film of $Co_{50}Fe_{50}/Ni_{80}Fe_{20}$. Chen *et al.* [21] reported the low field magnetostriction in an annealed Co-30% Fe alloy. Thick sheets of Co-Fe were bonded to a fibre Bragg grating sensor for magnetostriction measurements under different external magnetic fields. The majority of the studies concentrated on single mode fibers with an interferometer configuration for sensing the magnetic field. Further, the transducers were in the form of ribbons which were attached to the fibre using an epoxy. Long period grating based fibre sensors in combination with a thin film magnetostrictive transducer is a better alternative for sensing the parameters such as magnetic field and strain. A survey of the literature reveals that not much work has been done on exploring the possibilities of Metglas thin film-LPG based magnetostrictive sensors. The combined use of Metglas thin films and an external magnetic field can provide excellent tuning and chirping of long period fibre gratings. The integration of a magnetostrictive material to an optical fibre long period grating can thus find potential applications in magnetic field sensing, wavelength tunable optical filters and multiplexing devices. Therefore, the integration of Metglas thin films on to an optical fibre long period grating not only enable us in measuring magnetostriction of amorphous thin films but also help us in realizing possible magnetostrictive sensor devices.

The present work reports on the preparation of Metallic glass alloy Metglas 2826 MB based amorphous thin films and their integration into an optical fibre long period grating for potential magnetostrictive sensor applications. As prepared amorphous thin films were characterized using transmission electron microscopy and x-ray photoelectron spectroscopy. The film was coupled to a long period fibre grating. The attenuation band of the Metglas thin film coupled LPG had dependence on the strength of the magnetic field. Field dependent magnetostriction values were calculated from the shift in the central wavelength of the attenuation band. The results are presented here.

2. Experiment

Long Period Grating was realized by exposing a photosensitive fibre, Newport F-SBG-15 to an excimer laser operated at 248 nm. Point to point technique was used for writing the grating and the grating period was 575 μm. The grating was written over a length of 2 cm. Metglas thin films of thickness around 100 nm were deposited simultaneously onto a silicon substrate, NaCl substrate and an optical fibre long period grating, employing the thermal evaporation technique. Commercially available Metglas 2826 MB ribbon of composition $Fe_{40}Ni_{38}Mo_4B_{18}$ was employed as a source material to deposit thin films. The films were deposited by thermal evaporation using a current of 25 A at a base pressure of $1x10^{-5}$ mbar. A base pressure of ~ $1x10^{-5}$ mbar was achieved by a diffusion pump backed with a rotary pump. Transmission electron microscopy (TEM) experiments were carried out on films coated on NaCl substrates. A JOEL JEM-2200 FS electron microscope operated at 200 kV was used for this. The compositions of the films were analyzed using an energy dispersive x-ray spectrometer which was attached to the TEM column. X-ray photoelectron spectroscopy (XPS) measurements were carried out on films prepared on silicon substrates employing an Omicron Nanotechnology Multiprobe Instrument. XPS spectra were obtained using a high resolution hemisphere analyzer EA 125 HR equipped with a detection system consisting of seven channeltrons. A monochromatic Al Kα source of energy $h\nu$ = 1486.6 eV was used to probe the films which was attached to a molybdenum sample holder. Pressure in the XPS chamber during measurements was maintained at ~ 5×10^{-10} mbar. Room temperature magnetization measurements were carried out using a vibrating sample magnetometer (DMS 1660 VSM) with an external field varying from −2 to +2 kOe. Magnetostriction was measured by using an instrument with an optical fibre long period grating device, as shown in Fig. 1. A bar magnet (l=5 cm, b=1 cm and h=1 cm) was mounted with its long axis parallel to the optical fibre as shown in Fig. 1. The bar magnet was placed on a translation stage so that the position of magnet with respect to the optical fibre can be varied with a precision of 0.01 mm. In the present configuration, the magnetic field direction is parallel to the fibre axis and thus the field direction is along the easy magnetic axis of the deposited thin film. The magnetic field strength was measured using a hall probe attached to a gauss meter and the measured field ranged from 1370 gauss to 160 gauss when the distance between the bar magnet and optical fibre was varied from 3 mm to 20 mm. The measured magnetic fields were 1370, 1180, 1010, 500, 265 and 160 gauss for 3, 4, 5, 10, 15 and 20 mm distances. The transmission spectrum of the long period grating was recorded at different magnetic fields using an optical spectrum analyzer (YOKOGAWA, Model AQ6319) with a wavelength resolution of 10 pm. The source used for the spectral measurement was a Broad Band Source (BBS), Yokogawa AQ4305. In the transmission spectrum, which is a plot of intensity vs. wavelength, loss peaks were observed at resonant wavelength corresponding to the coupling of core mode to cladding mode. This loss peaks were shifted depending on the axial strain applied to fibre by the coated magnetostrictive material under different magnetic fields. The coupling wavelength of LPG was noted at different magnetic fields and magnetostriction was calculated from the shift in the coupling wavelength.

3. Results and discussions

3.1 Structure and composition

3.1.1 Transmission electron microscopy

Figure 2 shows a TEM bright field image of the as deposited films. One can clearly notice that the microstructure exhibits very poor contrast typical of an amorphous material. The electron diffraction pattern shown in figure 3 is characteristic of an amorphous material.

3.1.2 XPS Analysis

XPS survey scan was collected for films deposited on silicon substrate and is depicted in figure 4. The spectrum exhibits characteristics photoelectron lines of Fe and Ni. The survey scan also exhibited lines corresponding to the emission of Auger electrons (Ni LMM, Fe LMM). The peak positions of Ni LMM and Fe LMM were 641 eV and 784 eV respectively which is in line with the reported values [22]. Boron and molybdenum were not detected in the XPS survey scan. The absence of molybdenum and boron in XPS indicates that the film is deficient in boron and molybdenum. In XPS the relative sensitivity of Fe, Mo and B compared to Ni is 0.86, 0.64 and 0.06 respectively. The low sensitivity for B is due to the small photoionization cross section for boron. However we were able to detect Mo and B in Metglas 2826 MB ribbon (the source material used for evaporation). The spectrum for B 1s and Mo 3d acquired from Metglas ribbon is shown figure 5 (a) and 5 (b) respectively. B 1s line was centered on 189.4 eV. The peak positions of Mo $3d_{5/2}$ and Mo $3d_{3/2}$ were 228.1 eV and 231.25 eV respectively and the 3d doublet separation was 3.15 eV. The scan for B 1s and Mo 3d lines in thin films [figure 5(c) and 5 (d)] doesn't show these elements in thin films. Since the detection limit of XPS is in the range 0.1 to 1 atom% we attribute the absence of Mo and B peaks in the XPS to the absence of these elements in the film. Figure 6 shows an EDS profile from the prepared amorphous thin film. Energy dispersive x-ray analysis confirmed the presence of iron and nickel and the composition of the film was found to be $Fe_{55}Ni_{45}$.

3.2 Magnetic properties

Figure 7 shows room temperature hysteresis loop for thin film in parallel field. The saturation magnetization was found to be 865 emu/cc and the saturation was achieved at a field of 1000 Oe. The coercivity was ~ 60 Oe. Even in the absence of crystalline anisotropy, the origin of coercivity can be due to magnetoelastic anisotropies arising from stresses in the film.

In order to gain further insight into the magnetostrictive properties of the film, the magnetostriction was determined at various magnetic fields. The magnetostriction was measured by using an instrument with an optical fibre grating device, as shown in Fig. 1. The shift in the coupling wavelength due to the magnetostrictive strain was obtained with an optical spectrum analyzer.

For long period gratings, the energy typically couples from the fundamental guided mode to discrete, forward propagating cladding mode. The energy transferred to a cladding mode is then absorbed in the protective coating elsewhere in the fibre, which gives rise to an absorption band in the transmission spectrum of a fibre containing such a grating. The peak wavelength of absorption is defined by equation 1. When a tensile stress is applied to the optical fibre long period grating the periodic spacing changes and thereby causes the coupling wavelength to shift.

The axial strain sensitivity of LPG's [18] may be assessed by differentiating equation (1)

$$\frac{d\lambda}{d\varepsilon} = \frac{d\lambda}{d\left(\delta n_{eff}\right)}\left(\frac{dn_{eff}}{d\varepsilon} - \frac{dn_{cl}}{d\varepsilon}\right) + \Lambda\frac{d\lambda}{d\Lambda} \tag{2}$$

The sensitivity comprises the material effects i.e. the change in fibre dimension and the strain-optic effect as well as waveguide effects arising from the slope of the dispersion term $\frac{d\lambda}{d\Lambda}$.

When an axial strain is applied to a fibre grating, the resonant wavelength of the fibre grating will shift because the Λ of the grating will increase and at the same time the effective refractive index of both core and cladding modes will decrease due to the photoelastic effect of the fibre.

The amount of wavelength shift is given by [23]

$$\frac{\delta\lambda}{\lambda} = \gamma\frac{(1-p_{co})n_{eff} - (1-p_{cl})n_{cl}}{n_{eff} - n_{cl}}\varepsilon \tag{3}$$

Here p_{co} and p_{cl} are the elastooptic parameters of core and cladding correspondingly , n_{eff} and n_{cl} are the effective refractive indices of core mode and cladding mode, ε is the strain induced on the fibre grating and γ is a generalized sensing parameter which essentially represents a feedback due to the presence of the grating in dispersive fibre [24] **.** The values of p_{co} and p_{cl} are normally in the range 0.20 to 0.25 for silica fibre and for a simplified case one can assume $p_{co} \approx p_{cl} = p_e$ where p_e is the effective elastooptic parameter for silica. p_e is defined as

$$p_e = \left(n^2/_2\right)[P_{12} - \nu(P_{11} + P_{12})]$$

Here n is the refractive index of fused silica, υ is the Poisson ratio and P_{11} and P_{12} are the two strain optic coefficients.

The effective photoelastic parameter, p_e is about 0.22 for a silica fibre. Considering $\gamma \approx 1$ and the strain is homogeneous and isotropic, equation 3 simplifies to its more common form

$$\frac{\delta\lambda}{\lambda} = [1 - p_e]\varepsilon \cong 0.78\varepsilon \tag{4}$$

This allows the magnetostriction of the sample (ε_s) to be directly determined by [21]

$$\varepsilon_S = \left(\frac{l_f}{l_s}\right)\varepsilon = \left(\frac{l_f}{l_s}\right)\frac{1}{0.78}\frac{\delta\lambda}{\lambda} \qquad (5)$$

The factor $\left(l_f / l_s \right)$ is introduced to accommodate the difference in length between the fibre grating (l_f) and the sample (l_s). In the present experiment we have used l_f = 2 cm and l_s = 2 cm.

Figure 8 (a)-(e) shows the transmission spectra in the wavelength range 1625 nm-1665 nm of the Metglas thin film coated LPG for magnetic fields ranging from 160 gauss to 1370 gauss. The peak position was determined by fitting the experimental spectra using the Lorentzian function (red line in the transmission spectra).

Figure 8(f) shows resonance wave length versus applied magnetic field. For magnetic fields in the range 160 gauss to 500 gauss the change in the resonance wavelength was minimal. Possible reasons can be the insensitiveness of the fibre grating to very small strains or the changes if any may be less than the resolution of the spectrometer. There is a decrease in the resonance wavelength position from 1643.34 nm to 1643.17 as the magnetic field increases from 500 gauss to 1180 gauss. For higher magnetic fields the change is minimal since the film has reached its magnetic saturation (figure 7).

Magnetostriction values calculated at different fields using the equation (5) are shown in figure 9. The saturation magnetostriction was found to be ~ 130 ppm and the magnetostriction was saturated at fields of ~ 1200 gauss. Two points are to be noted here; 1) magnetostriction values presented in figure 9 corresponds to that for a metglas thin film/silica fibre system rather than that for a free standing metglas thin film and 2) magnetostriction values presented here are based on the assumption that the strain induced on film and fibre are equal in magnitude. In an ideal case one should also consider the elastic properties of both transducer and sensor while calculating the magnetostriction [25, 26]

The origin of magnetostriction in amorphous ferromagnetic materials has been addressed previously [27]. In macroscopically isotropic amorphous feromagnets the average magnetic anisotropy is zero. However the material can be considered as consisting of very small structural units with strong uniaxial anisotropy and with easy axis varying randomly from site to site. These structural units exhibit spontaneous magnetostrictive strains, like small crystalline ferromagnets with corresponding orientation of easy axes [27]. The units are mechanically coupled and the macroscopic strain manifests itself by elastic strain transfer from one unit to another. The summation of these elastic strains is non-zero due to the anisotropic elastic properties of the structural units [28].

Coupling of magnetostriction in Metglas thin films with long period fibre grating shows the applicability of this device for magnetic field sensors as well as for position sensing applications. The use of optical fibre for magnetic field sensing offers many advantages compared to its electronic counterpart, such as remote sensing, multiplexing different point sensors on a single fibre and sensing under hazardous conditions. It will be worth comparing the saturation magnetostriction in the present experiment with previously reported ones. The saturation magnetostriction of 130 ppm is comparable with the observations of Chen *et al.* [21] in annealed Co-Fe samples. But the field required for saturation in the present experiment is much larger (~ 1200 gauss) than the reported one (~600 gauss). Saturation magnetostriction of thin films in the present case is much larger than the magnetostriction exhibited by Metglas 2826 MB ribbons which is ~ 12 ppm . What is evident here is that from a material point of view, the thin film form of metallic glass alloy Metglas 2826 MB is promising for magnetostriction applications due to their comparable saturation magnetostriction with the bulk counterparts. But from a device point of view, improvements are necessitated. The shift in the LPG spectrum with an external magnetic field is small and high resolution spectrometers are necessary for detecting it. A fibre grating with good axial sensitivity will be a better choice from an application point of view. Further, scope exists in amplifying the strain, for e.g. by using a multilayer stack of alternative magnetostrictive material (Metglas) and a non-magnetic thin film and a variety of applications such as wavelength tunable optical signal filter, wavelength channel add/drop multiplexer or a signal compensator is possible. Even though optimizations are required from an application point of view, the present study was successful in demonstrating a novel way to explore magnetostriction in metallic glass thin films.

4. Conclusions

Metglas 2826 MB based amorphous thin films were prepared by the thermal evaporation technique. Transmission electron microscopy studies showed the amorphous nature of the sample. The presence of iron and nickel were established using x-ray photoelectron spectroscopy and energy dispersive x-ray spectroscopy techniques. The film was integrated to a long period fibre grating. The central wavelength of the attenuation band in the transmission spectrum of the long period grating decreased with an increase in the magnetic field. This dependence was due to the transfer of strain from film to fibre on application of a magnetic field. The change in the resonance wavelength was minimal once the film achieved its magnetic saturation. The magnetostriction properties exhibited by this film imply the potential application of this material in magnetostrictive sensor devices.

Acknowledgement

This work is supported by Inter University Accelerator Centre, New Delhi through UGC Funded University project UFUP No. 35306. Senoy Thomas acknowledges CSIR, New Delhi for Senior Research Fellowship. RVR acknowledges support from SERC, Singapore through grant 0621010032.

References

1. A. Kolano-Burian, R. Kolano, M. Kowalczyk, J. Szynowski, M. Steczkowska-Kempka, T. Kulik, Structure and magnetic properties of magnetostrictive rapidly-quenched alloys for force sensors applications, J. Phys.: Conf. Ser. 144 (2009) 012062 1-4
2. A.G. Olabi, A. Grunwald, Design and application of magnetostrictive materials, Mater Des. 29 (2008) 469-483
3. J.Lou, R. E. Insignares, Z. Cai, K. S. Ziemer, M. Liu and N. X. Sun, Soft magnetism, magnetostriction, and microwave properties of FeGaB thin films, Appl. Phys. Lett. 91 (2007) 182504 1-3
4. E.Hristoforou, Magnetostrictive delay lines: engineering theory and sensing applications, Meas. Sci. Technol. 14 (2003) R15-R47
5. Dimitrios Kouzoudis, Dionysios E. Mouzakis, A 2826 MB Metglas ribbon as a strain sensor for remote and dynamic mechanical measurements, Sens. Actuators, A, 127 (2006) 355-359
6. Ee Lim Tan, Brandon D. Pereles, Ranyuan Shao, Justin Ong, Keat Ghee Ong, A wireless, passive strain sensor based on the harmonic response of magnetically soft materials, Smart Mater. Struct., 17 (2008) 025015 1-6
7. Wen Shen, Ramji S. Lakshmanan, Leslie C. Mathison, Valery A. Petrenko, Bryan A. Chin, Phage coated magnetoelastic micro-biosensors for real-time detection of Bacillus anthracis spores, Sens. Actuators, B, 137 (2009) 501-506
8. M. R. J. Gibbs, E. W. Hill, P. J. Wright, Magnetic materials for MEMS applications, J. Phys. D: Appl. Phys. 37 (2004) R237-R244.
9. M. R. J. Gibbs, Materials Optimization for Magnetic MEMS, IEEE Trans. Magn. 43 (2007) 2666-2671
10. M. Jyothi, C. Suryanarayana, Structure of vapour deposited METGLAS 2826 MB films, Z. Metallkd. 76 (1985) 802-805
11. T. Hysen, S. Deepa, S.Saravanan, R.V.Ramanujan, D.K.Avasthi, P.A.Joy, S.D.Kulkarni, M. R. Anantharaman, Effect of thermal annealing on $Fe_{40}Ni_{38}B_{18}Mo_4$ thin films: modified Herzer model for magnetic evolution, J. Phys. D: Appl. Phys. 39 (2006) 1993

12. Senoy Thomas, S. H. Al-Harthi, D. Sakthikumar, I. A. Al-Omari, R. V. Ramanujan, Yasuhiko Yoshida, M. R. Anantharaman, Microstructure and random magnetic anisotropy in Fe–Ni based nanocrystalline thin films, J. Phys. D: Appl. Phys. 41 (2008) 155009 1-8.
13. Senoy Thomas, S. H. Al-Harthi, R.V.Ramanujan, Zhao Bangchuan, Liu Yan; Wang Lan, M. R.Anantharaman, Surface evolution of amorphous nanocolumns of Fe–Ni grown by oblique angle deposition, Appl. Phys. Lett. 94 (2009) 063110 1-3.
14. Senoy Thomas, Hysen Thomas, D. K. Avasthi, A. Tripathi, R. V. Ramanujan, M. R.Anantharaman, Swift heavy ion induced surface modification for tailoring coercivity in Fe-Ni based amorphous thin films, J. Appl. Phys. 105 (2009) 033910 1-7.
15. Senoy Thomas, S. H. Al-Harthi, I. A. Al-Omari, R. V. Ramanujan, V. Swaminathan, M. R. Anantharaman, Influence of substrate topography on the growth and magnetic properties of obliquely deposited amorphous nanocolumns of Fe–Ni, J. Phys. D: Appl. Phys.42 (2009) 215005 1-8
16. Alan D. Kersey, Michael A. Davis, Heather J. Patrick, Michel LeBlanc, K. P. Koo, C. G. Askins, M. A. Putnam, E. Joseph Friebele, Fiber grating sensors, J. Lightwave Technol. 15 (1997) 1442-1463
17. Kenneth O. Hill, Gerald Meltz, Fiber Bragg Grating Technology Fundamentals and Overview, J. Lightwave Technol. 15 (1997) 1263-1276
18. Stephen W James, Ralph P Tatam, Optical fibre long-period grating sensors: characteristics and application, Meas. Sci. Technol 14 (2003) R49-R61
19. Miroslav Sedlar, Ivan Paulicka, Michael Sayer, Optical fiber magnetic field sensors with ceramic magnetostrictive jackets, Appl. Optics. 35 (1996) 5340-5344
20. S.Rengarajan, R. M. Walser, High-speed fiber-optic sensor for magnetic-field mapping, J. Appl. Phys. 81 (1997) 4278-4280
21. L. H. Chen, T. J. Klemmer, H. Mavoori, S. Jin, Low-field magnetostriction in an annealed Co–30% Fe alloy, Appl. Phys. Lett 74 (1999) 2047-2049

22. J F Moulder, W F Stickle, P E Sobol, K D Bomben, Handbook of X-ray Photoelectron Spectroscopy, Perkin-Elmer, Minnesota, 1992, p 80, 84
23. YUAN Yin-quan, LIANG Lei and ZHANG Dong-sheng, Spectra of fiber Bragg grating and long period fiber grating undergoing linear and quadratic strain, Optoelectron. Lett. 5 (2009) 182-185
24. J. S. Petrovic, V. Mezentsev, H. Dobb, D. J. Webb, K. Kalli, I. Bennion, Multiple period resonances in long period gratings in photonic crystal fibres, Opt Quant Electron. 38 (2006) 209–216
25. I. Carabias, A. Martinez, M.A. Garcia, E. Pina, J.M. Gonzalez, A. Hernando, P. Crespo, Magnetostrictive thin films prepared by RF sputtering, J. Magn. Magn. Mater. 290-291 (2005) 823-825
26. Stefan Schmidt, Craig A. Grimes, Characterization of nano-dimensional thin-film elastic moduli using magnetoelastic sensors, Sens. Actuators, A, 94 (2001) 189-196
27. M. Fähnle, J. Furthmüller, G. Herzer, Theory of magnetostriction in amorphous ferromagnets, J. Phys. Colloques 49 (1988) 1329-1330
28. M. R. J. Gibbs, Anisotropy and magnetostriction in amorphous alloys, J. Magn. Magn. Mater. 83 (1990) 329-333

Biographies

Mr. Senoy Thomas did his doctoral research in the Department of Physics, Cochin University of Science and Technology, India during the year 2005-2009. Presently he is a research fellow in the Institute for Physics, Technical University of Chemnitz, Germany. He obtained his masters in Physics from Mahatma Gandhi University, Kottayam, India. Later on he joined Cochin University of Science and Technology, Cochin, India and obtained a masters degree in Philosophy in 2005. He is also a recipient of Senior Research Fellowship from Council of Scientific and Industrial Research, Government of India. His research interest includes amorphous and nanocrystalline magnetic materials, sol-gel synthesis of nanocomposites, ion beam modification of materials and characterizing nano materials using state of the art techniques.

Mr. Jinesh Mathew is presently a doctoral student at DIT Photonics Research Centre of Dublin Institute of Technology, Dublin, Ireland. His area of research is fibre optic sensors. He obtained his Master of Philosophy, M Phil. in Photonics and Master of Science, M Sc. in Electronics from Cochin University of Science and Technology, Cochin, India. During his masters programme he succeeded in developing a biopolymer based fibre optic humidity sensor. His research interests are in fibre optic sensors, photonic crystal fibers, fiber gratings and bio-sensors.

Prof. P. Radhakrishnan is currently the director of Centre of Excellence in Lasers and Optoelectronic Sciences at Cochin University of Science and Technology, Cochin, India. He received his Ph.D. degree from Cochin University of Science and Technology in 1986. Presently he is a Professor at the International School of Photonics, Cochin University of Science and Technology. His research interests include laser technology, laser spectroscopy, and fiber optic sensors.

Dr. V P N Nampoori is a Professor of Photonics in International School of Photonics, Cochin University of Science and Technology. He took his Ph D in Physics in the field of Molecular Spectroscopy. At present he is working in topics related to Lasers, Photonics and Nonlinear Dynamics. Dr. Nampoori has published more than 300 research papers and guided about 15 PhDs in lasers, laser spectroscopy and fibre optics. Significant contributions of Dr Nampoori are in the area of Fibre optic Sensors, Nonlinear Optics and Photonic materials.

Dr. A K George graduated with MSc. and PhD. (1980) in Applied Physics from the Faculty of Technology and Engineering, M.S. University of Baroda, India. Later, he did post-doctoral research at Chelsea College of Science and Technology (now part of King's College), University of London. Subsequently he worked at Bayero University, Nigeria before joining Sultan Qaboos University (SQU) as Assistant Professor in 1987.

Dr. Salim Al-Harthi is presently an Associate Professor at the department of physics, Sultan Qaboos University (SQU), Muscat, Sultanate of Oman. He received his Ph.D. degree from Warwick University in 2001 for a thesis titled "Depth Profiling of Ultra-Shallow Implants in Silicon". His research interests are on two main areas: Surface/interface physics and nanotechnology.

Dr. Raju V Ramanujan is presenly an Associate Professor in the School of Materials Science and Engineering, Nanyang Technological University, Singapore. Dr. Ramanujan received his Master of Engineering and Ph.D. degree in Materials Science at Carnegie Mellon University (CMU). At CMU he was the recipient of a Fellowship from a U.S. National Science Foundation grant. He earned his Bachelor's degree (First Class Honors) from Indian Institute of Technology, Bombay. The focus of research in Dr. Ramanujan's group is the study and development of advanced nanomaterials, especially magnetic nanomaterials for energy, bioengineering, information storage and defense applications.

Prof. M R Anantharaman is presently the head of the department of physics of the Cochin University Science and technology, Cochin, India. His Interests include nanomagnetic materials, magnetic nano composites, magnetic elastomers, ferrofluids and conducting polymers. He received his Ph.D degree from the Indian Institute of Technology, Bombay, India in 1985. He also worked at the Technical University of Eindhoven, The Netherlands as a Post-Doctoral Fellow for a year during 1993-94 on a BOYSCAST Fellowship awarded by the Government of India. He is also a visiting professor at the University of Konstanz, Germany and Sultan Qaboos University, Muscat, Sultanate of Oman.

Figure Captions

1) **Figure 1.** Schematic of the experimental set up for measuring magnetostriction
2) **Figure 2.** TEM bright field image of vapor deposited Metglas thin film.
3) **Figure 3.** Electron diffraction pattern of vapor deposited Metglas thin film.
4) **Figure4.** XPS survey scan for Metglas based thin film
5) **Figure 5. (a)** B 1s spectrum of the source material used for evaporation (Metglas 2826 MB ribbon) (b) Mo 3d of the source material used for evaporation (Metglas 2826 MB ribbon) (c) XPS scans for B 1s in thin films and (d) XPS scans for Mo 3d in thin films
6) **Figure 6**. EDS profile of Metglas based thin films
7) **Figure 7.** Room temperature M-H curve for Metglas film in a parallel field
8) **Figure 8.** (a) LPG Transmission spectrum at a magnetic field of 160 gauss (b) 500 gauss (c) 1010 gauss (d) 1180 gauss and (e) 1370 gauss. Variation of peak position with applied magnetic field is shown in (f)
9) **Figure 9.** Magnetostriction coefficient for Metglas films at different magnetic fields

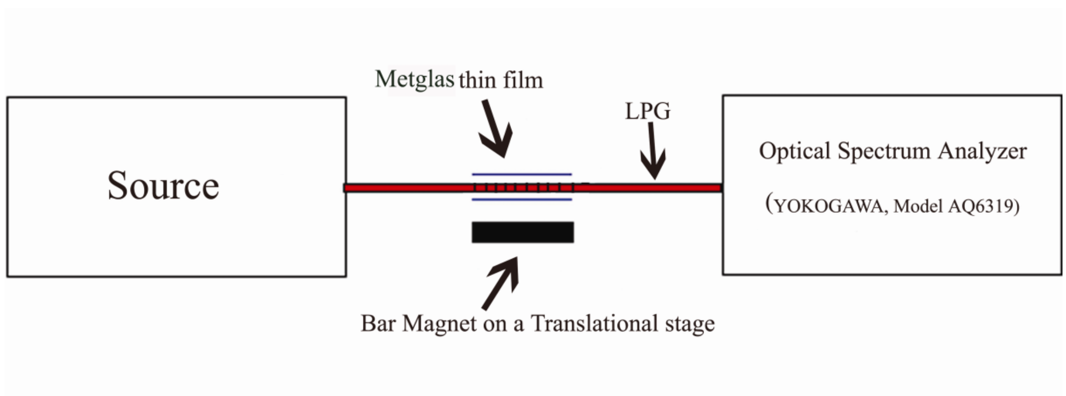
Metglas thin film
LPG
Source
Optical Spectrum Analyzer
(YOKOGAWA, Model AQ6319)
Bar Magnet on a Translational stage

Figure 1

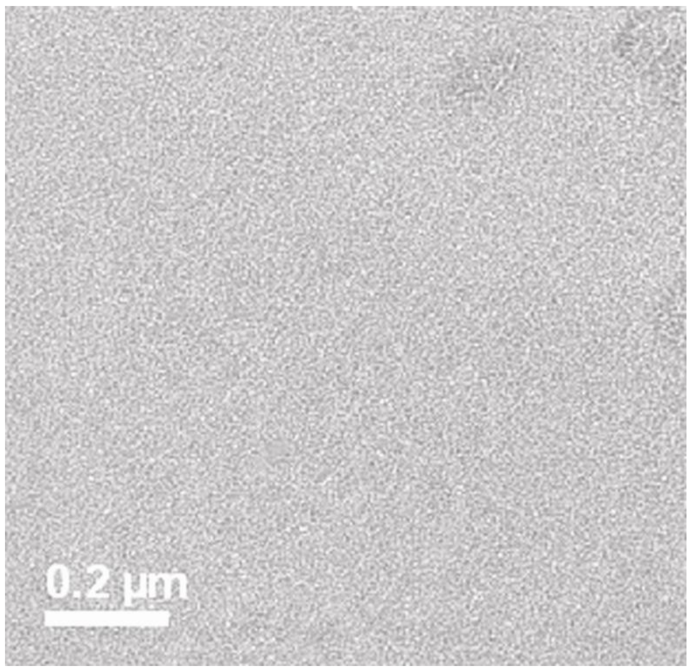

Figure 2

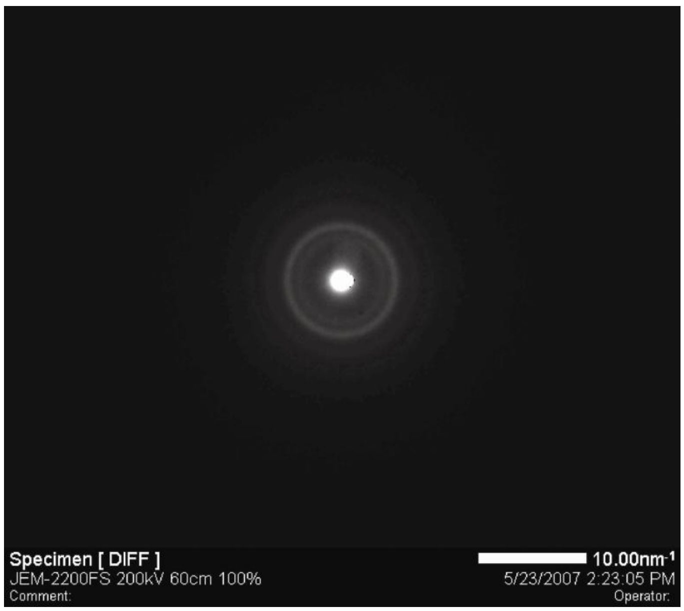
Specimen [DIFF]
JEM-2200FS 200kV 60cm 100%
Comment:
10.00nm-1
5/23/2007 2:23:05 PM
Operator:

Figure 3

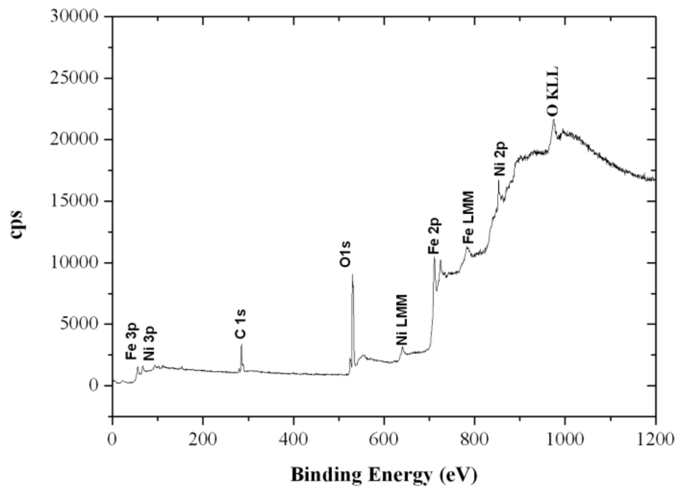

30000
25000
20000
15000
10000
5000
0
cps
0
200
400
600
800
1000
1200
Binding Energy (eV)
Fe 3p
Ni 3p
C 1s
O1s
Ni LMM
Fe 2p
Fe LMM
Ni 2p
O KLL

Figure 4

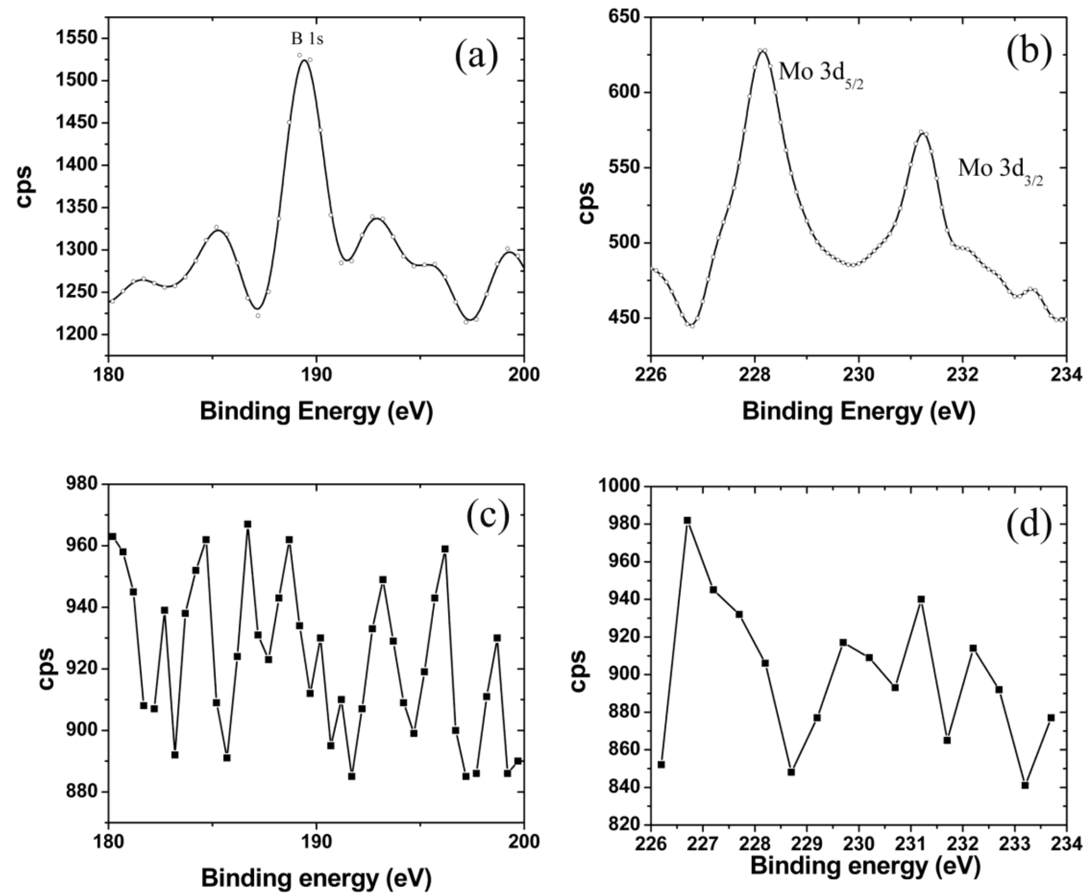
(a)
B 1s
cps
Binding Energy (eV)
(b)
Mo 3d5/2
Mo 3d3/2
cps
Binding Energy (eV)
(c)
cps
Binding energy (eV)
(d)
cps
Binding energy (eV)

Figure 5

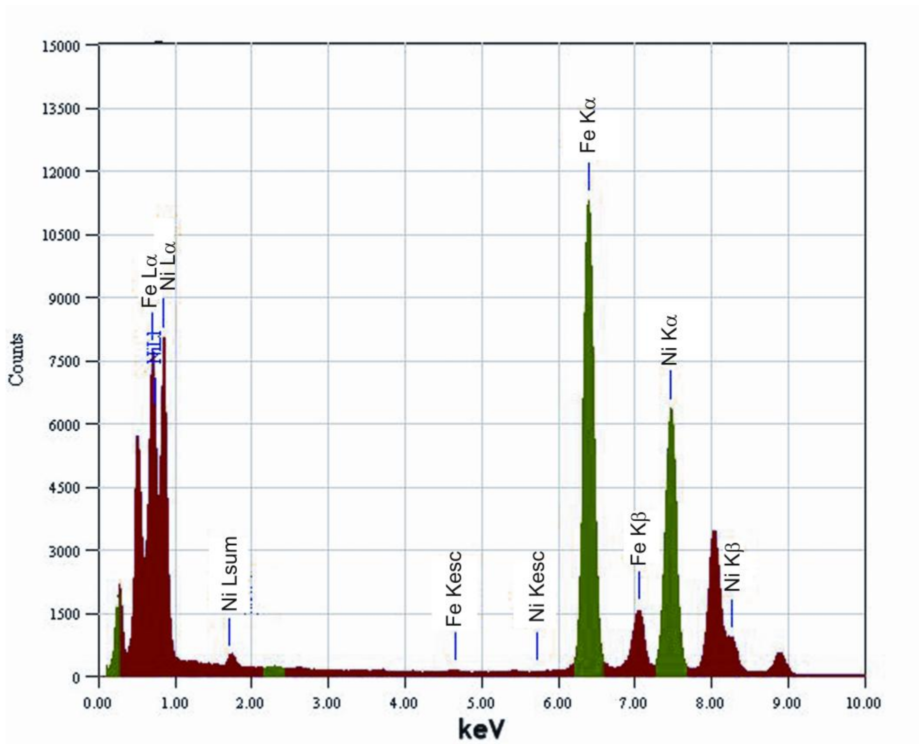
15000
13500
12000
10500
9000
7500
6000
4500
3000
1500
0
Counts
0.00
1.00
2.00
3.00
4.00
5.00
6.00
7.00
8.00
9.00
10.00
keV
Fe Lα
Ni Lα
Ni Lsum
Fe Kesc
Ni Kesc
Fe Kα
Fe Kβ
Ni Kα
Ni Kβ

Figure 6

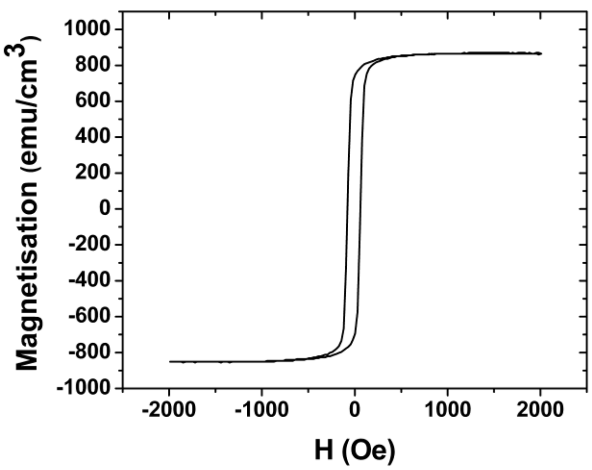
Magnetisation (emu/cm3)
1000
800
600
400
200
0
-200
-400
-600
-800
-1000
-2000
-1000
0
1000
2000
H (Oe)

Figure 7

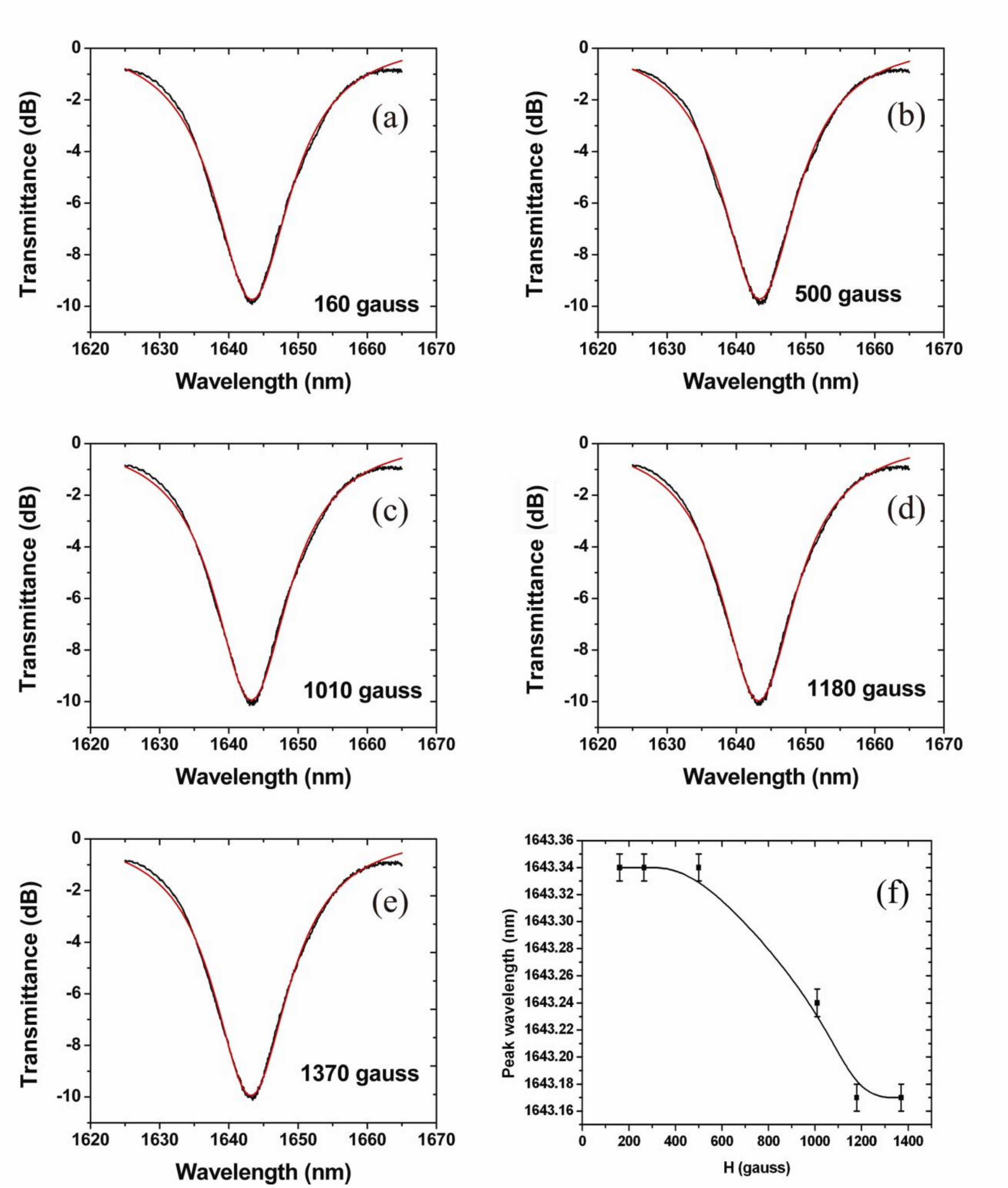
(a)
160 gauss
(b)
500 gauss
(c)
1010 gauss
(d)
1180 gauss
(e)
1370 gauss
(f)
Transmittance (dB)
Wavelength (nm)
Peak wavelength (nm)
H (gauss)

Figure 8

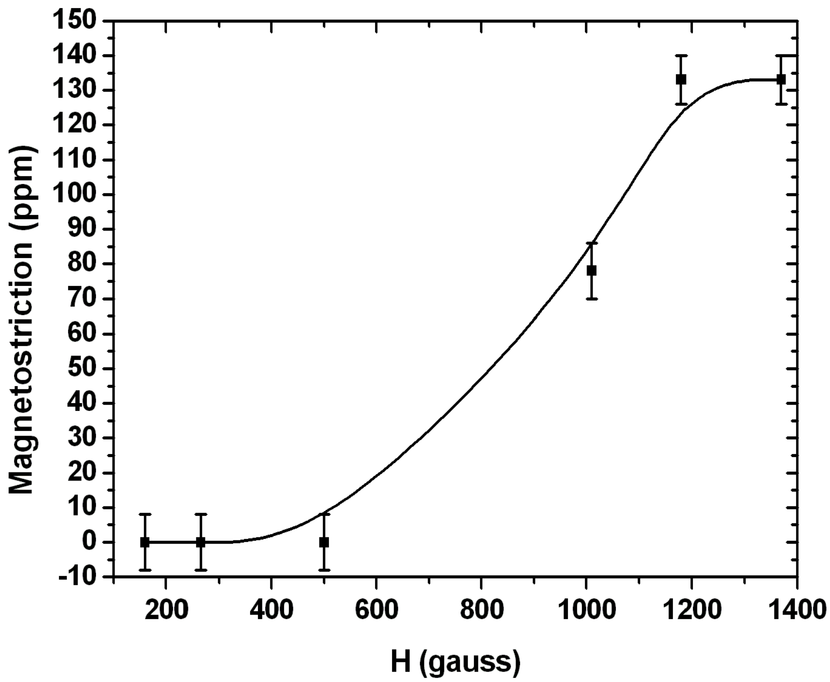
150
140
130
120
110
100
90
80
70
60
50
40
30
20
10
0
-10
Magnetostriction (ppm)
200
400
600
800
1000
1200
1400
H (gauss)

Figure 9